Environmental Science & Technology

pubs.acs.org/est

Article

Atmospheric Photosensitization: A New Pathway for Sulfate Formation

Xinke Wang, Rachel Gemayel, Nathalie Hayeck, Sebastien Perrier, Nicolas Charbonnel, Caihong Xu, Hui Chen, Chao Zhu, Liwu Zhang, Lin Wang, Sergey A. Nizkorodov, Xinming Wang, Zhe Wang, Tao Wang, Abdelwahid Mellouki, Matthieu Riva, Jianmin Chen,* and Christian George*

Cite This: *Environ. Sci. Technol.* 2020, 54, 3114−3120

Read Online

ACCESS | Metrics & More | Article Recommendations | Supporting Information

ABSTRACT: Northern China is regularly subjected to intense wintertime "haze events", with high levels of fine particles that threaten millions of inhabitants. While sulfate is a known major component of these fine haze particles, its formation mechanism remains unclear especially under highly polluted conditions, with state-of-the-art air quality models unable to reproduce or predict field observations. These haze conditions are generally characterized by simultaneous high emissions of SO_2 and photosensitizing materials. In this study, we find that the excited triplet states of photosensitizers could induce a direct photosensitized oxidation of hydrated SO_2 and bisulfite into sulfate S(VI) through energy transfer, electron transfer, or hydrogen atom abstraction. This photosensitized pathway appears to be a new and ubiquitous chemical route for atmospheric sulfate production. Compared to other aqueous-phase sulfate formation pathways with ozone, hydrogen peroxide, nitrogen dioxide, or transition-metal ions, the results also show that this photosensitized oxidation of S(IV) could make an important contribution to aerosol sulfate formation in Asian countries, particularly in China.

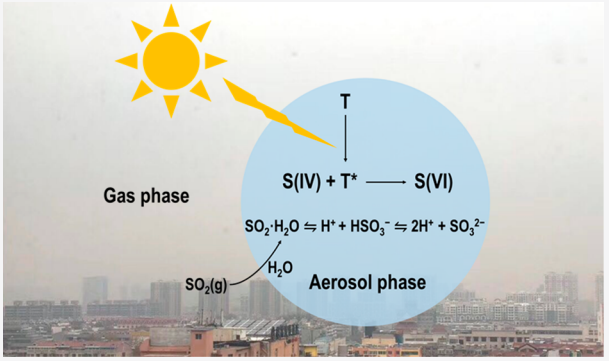

INTRODUCTION

Fine particulate matter, a complex cocktail of inorganic and organic species, has a central role during persistent haze events in the North China Plain. While sulfate (SO_4^{2-}) is ubiquitous and a key component, its production from SO_2 is still uncertain. While gaseous SO_2 can be oxidized through its reaction with OH radicals, it also undergoes significant multiphase processing through reactions involving a variety of dissolved oxidants such as ozone (O_3), hydrogen peroxide (H_2O_2), and transition-metal ions (TMIs).[1−3] However, the detailed chemical mechanism under heavily polluted conditions remains uncertain. Current atmospheric observations highlighting high sulfate production during severe haze events[4] cannot be reproduced by atmospheric models.[5] To close this gap, new chemical pathways have been suggested involving an interfacial SO_2 oxidation on acidic microdroplets,[6] SO_2 triplet state chemistry,[7−9] or oxidation at higher pH via a reaction with NO_2.[10,11] In sum, despite intense research efforts, important missing processes hamper our abilities to clearly elucidate the formation of one of the most important components of haze particles.

Photosensitized chemistry has been recently discussed as triggering novel chemistry in tropospheric particles,[12] but its role in S(IV) oxidation under polluted conditions has not been explored. A photosensitizing molecule will absorb solar radiation and create an excited (triplet) state T* from which various chemical pathways can be initiated that would otherwise not take place at the ground state.[13] Biomass burning for residential heating, typical for China during haze events, is in fact a likely source of compounds bearing functional groups capable of photosensitized oxidation as observed in humic-like substances (HULIS).[14] We therefore investigated whether photosensitized oxidation of SO_2 may occur under atmospheric conditions, as an attempt to close some gaps in our knowledge of sulfate formation under polluted conditions.

MATERIALS AND METHODS

All experiments were conducted at room temperature in the range of 295−300 K.

Chemicals. All chemicals were used as purchased: acetophenone (Sigma Aldrich, 98%), flavone (Sigma Aldrich, ≥99.0%), xanthone (Sigma Aldrich, 97%), 4-(benzoyl)benzoic acid (4-BBA, Sigma Aldrich, 99%), sodium sulfite (Sigma Aldrich, ≥98%), sulfuric acid (Sigma Aldrich, 95−97%), humic acid (HA, Sigma Aldrich, technical grade), humic acid salt

Received: October 22, 2019
Revised: January 30, 2020
Accepted: February 5, 2020
Published: February 5, 2020

(HAS, Sigma Aldrich, technical grade). In addition, all solutions were freshly prepared using ultrapure water (Elga Purelab Classic, 18.2 MΩ cm). In order to promote dissolution, 4-BBA solutions were stirred in an ultrasonic bath for 10 min, and the solutions of xanthone and flavone were agitated for 2 h in the dark, both at ambient temperature. For the chromatographic analysis, acetonitrile, water, and formic acid were all of Optima LC/MS grade, provided by Fisher Scientific. *O*-(2,3,4,5,6-Pentafluorophenyl) methylhydroxyl amine hydrochloride (PFBHA, ≥99.0%) was purchased from Fluka. In addition, SO_2 (10 ppm, mixing with pure N_2, Linde, France) and N_2 (99.999%) were used in this study.

$PM_{2.5}$ Sample Collection and Extraction. 24 h ambient aerosol samples ($PM_{2.5}$ masses in the range of 27−46 mg) were collected onto 90 mm prebaked quartz-fiber filters (Whatman Company, UK) during December 10 to 14, 2018 using a midvolume sampler (TH-150A, Wuhan Tianhong, China) operating at 100 L min^{-1}. The sampling site was located in rural Wangdu (38°42′ N, 115°08′ E), Baoding, Hebei Province, surrounded by grasslands and farms, but easily influenced by industrial and urban plumes from megacities such as Beijing, Tianjin, and Shijiazhuang. After sampling, filters were stored at −20 °C in a freezer before further analysis.

Each quartz filter was extracted with three subsequent 15 mL extractions of ultrapure water and agitated for 25 min on an orbital shaker set at 1000 rpm. After filtering through a 0.2 μm polytetrafluoroethylene membrane (13 mm, Pall Corp., USA) using a glass syringe, the combined ambient aerosol extracts (AA as the abbreviation) were used to conduct the photochemical experiments described below. In addition, in order to characterize chromophores and carbonyl-containing compounds, these extracts were analyzed by using a UPLC/DAD/(+/−)HESI-HRMS platform, which is the combination of ultra-high performance liquid chromatography (UPLC, Dionex 3000, Thermo Scientific, USA), a diode array detector (DAD), and an Orbitrap high-resolution mass spectrometer (HRMS, Q Exactive, Thermo Scientific, Bremen, Germany) using heated electrospray ionization (HESI). More information about chemical analysis of filter samples is illustrated in the Supporting Information.

Quartz Cell Experiments. A 14 mL cylindrical quartz cell (5 cm length and 2 cm diameter) mounted 13 cm away along its axis onto a xenon lamp (150 W; LOT-QuantumDesign, France) was used to perform the experiments. A quartz water filter of 5 cm length and a Pyrex filter were mounted in front of the lamp to remove infrared irradiation and short wavelengths ($\lambda < 290$ nm). The spectral characteristics of this system can be found in Figure 5 of Ciuraru et al.[15] In order to maximize the surface to volume ratio (1.4 cm^2 cm^{-3}), the cell was half-filled with 7 mL of pure water, 75 μM 4-BBA, 70 mg L^{-1} HA, 70 mg L^{-1} HAS, or AA (diluted by adding 1 mL ultrapure water or water acidified with sulfuric acid (H_2SO_4) to a desired pH, see below). An incoming diluted SO_2 gas flow (around 83 ppb after diluting by pure air) with a flow rate of 300 mL min^{-1} was injected through the cell, further diluted by adding 200 mL min^{-1} N_2, and then analyzed afterward using a SO_2 analyzer (Thermo, 43i). At the beginning of all experiments, higher concentrations of SO_2 were injected into the reactor in order to more rapidly reach the SO_2 gas/liquid equilibrium. In other words, these solutions were preconditioned with flowing gaseous SO_2 to establish Henry's law and acid−base equilibria, producing hydrated SO_2, HSO_3^-, and SO_3^{2-}, according to eqs 1−3:

$$SO_{2\,(g)} \rightleftharpoons SO_{2\,(aq)} \quad (1)$$

$$SO_{2\,(aq)} + H_2O \rightleftharpoons HSO_3^- + H^+ \ (pK_a \approx 1.88 \text{ at } 298K) \quad (2)$$

$$HSO_3^- \rightleftharpoons SO_3^{2-} + H^+ \ (pK_a \approx 7.22 \text{ at } 298K) \quad (3)$$

Sulfate concentrations in the liquid phase were measured using ion chromatography (IC, Metrohm, 881 Compact IC Pro - Anion, Switzerland). H_2SO_4 was added to adjust the pH of HA, HAS, and AA1 solutions, which were 4.0, 4.6, and 4.6, respectively. The pH values of 4-BBA and AA2 solutions were 4.4 and 6.2, respectively, without adding H_2SO_4. Due to the high pH of the AA2 solution, SO_2 concentrations in the gas/liquid phase did not reach the equilibrium even after injecting higher concentrations of SO_2 for over an hour. In addition, the 4-BBA solutions were degassed by bubbling pure N_2 around 30 min at a flow rate of 25 mL min^{-1}, which was also used to conduct the same experiment. Meanwhile, the incoming N_2 instead of pure air went through the quartz cell continuously. In all these experiments, the solutions were irradiated for 50 min, except for pure water (irradiated for 40 min).

Aerosol Flow Tube Experiments. Experiments were carried out at atmospheric pressure by using a horizontal jacketed aerosol flow tube (AFT, 6 cm internal diameter and 180 cm length) made of Pyrex. The air flowing through the reactor was kept at a constant temperature of 293 ± 1 K by means of a circulating water bath. There are five UV lamps (Cleo, Philips, Netherlands) surrounding the flow tube with a continuous emission spectrum over 300−420 nm and total irradiance from 0.75×10^{15} to 3.77×10^{15} photon cm^{-2} s^{-1}.[16] 4-BBA aerosols were generated from an aqueous solution (0.15 mM) by means of a constant-output atomizer (TSI model 3076). A portion of the aerosol flow (~0.33 L min^{-1}) was dried using a silica gel diffusion dryer, and monodispersed particles with diameters of 70 or 80 nm were selected for analysis with a differential mobility analyzer (DMA, TSI model 3081, impactor size 0.0508 cm), then mixed with SO_2 gas (22 mL min^{-1}, ~630 ppb after mixing), and injected into the AFT. The relative humidity measured at the outlet of the AFT was in the range of 25−27%. Seed particle concentration was approximately 800 particles cm^{-3}, and the residence time was ~15 min. A compact time-of-flight aerosol mass spectrometer (AMS, Aerodyne Inc.) was used to sample and analyze aerosols upon exiting the AFT. The obtained mass spectra were analyzed by using the AMS analysis software Squirrel version 1.60P and Pika version 1.20P. Water particles instead of 4-BBA particles were used as control experiments. During the control experiments, the silica gel diffusion dryer was moved from its normal position in front of the AFT to a position downstream from the AFT and in front of the AMS to allow water particles to enter the AFT without evaporation. In addition, all water particles were injected into the AFT without being size-selected.

Pulsed Laser Excitation Experiments. The transient absorption spectra of the excited acetophenone, flavone, xanthone, 4-BBA, and HULIS (extracted from the ambient aerosols) were measured using a pump−probe system described earlier,[17] and the experimental setup is shown in Figure S1. The third harmonic (266 nm, pulse width ~7 ns) of a Nd:YAG laser (Surelite II 10, Continuum) was used as an excitation source, operating in a single-shot mode. During these experiments, the laser pulse energy was limited to 10 mJ per pulse (~6 mJ cm^{-2}) in order to reduce the undesirable photolysis of the photo-

https://dx.doi.org/10.1021/acs.est.9b06347
Environ. Sci. Technol. 2020, 54, 3114−3120

sensitizer and avoid possible interferences from products. To avoid any interference or electron transfer with oxygen, the photosensitizer solutions were deoxygenated by bubbling argon through them for at least 20 min. The setup and principle of the pulsed laser system are described in detail in the Supporting Information.

For the kinetic measurements, the probe wavelengths for the transient absorption decays of the acetophenone, flavone, xanthone, and 4-BBA triplet states were 360, 350, 590, and 560 nm, respectively, which were around the corresponding maxima in the transient absorption spectra. T* extracted from the ambient aerosols had strong absorption in the wavelengths of 460, 480, and 500 nm, which were employed and averaged for kinetic measurements. Typically, signals from 30 repeated pulses were averaged for each observation wavelength.

All experiments were conducted under pseudo-first-order conditions due to a large excess of the quencher (i.e., S(IV)) compared to the initial photosensitizer concentrations. The absorption decay traces of the photosensitizer triplet state were fitted well with a single exponential process:

$$y = a + be^{-k_1 t} \tag{4}$$

where k_1 (s^{-1}) is the pseudo-first-order rate constant obtained from the slope of a logarithmic plot of the transient signals, and a reflects the potential deviation of the baseline after excitation (i.e., the absorption does not return to zero when absorbing products are produced). The lifetime of T* was defined as

$$\tau = \frac{1}{k_1} \tag{5}$$

In the bulk aqueous experiments in this study, in order to investigate the reactivities of hydrated SO_2 and HSO_3^- with T*, the sodium sulfite solution was added into the photosensitizer solutions, and then the pH of the solutions was decreased to 1.8 or 2.6 by adding a H_2SO_4 solution. Under these conditions, S(IV) existed mainly as hydrated SO_2 and HSO_3^-. The quenching rate coefficients for T* in the presence of S(IV) were determined by the Stern−Volmer equation (eq 6):

$$-\frac{d[T^*]}{dt} = (k_0 + k_{q(SO_2\cdot H_2O)}[SO_2\cdot H_2O] + k_{q(HSO_3^-)}[HSO_3^-])[T^*] = k_{obs}[T^*] \tag{6}$$

where k_0 corresponds to the rate coefficient of T* decay in the absence of oxygen or other quenchers, and $k_{q(SO_2\cdot H_2O)}$ and $k_{q(HSO_3^-)}$ are the rate coefficients for the quenching by hydrated SO_2 and HSO_3^-, respectively. It is important to underline that these rate constants are dependent on temperature and also pH.

RESULTS

Figure 1A shows the effect of such chemistry at 295−300 K, the diluted SO_2 gas flowing through a 14 mL reactor filled halfway with aqueous solutions containing different photosensitizers and illuminated with light-simulating actinic irradiation (λ > 290 nm). Various types of atmospherically relevant photosensitizing chemicals were used, namely, 4-(benzoyl)benzoic acid (4-BBA), humic acids and their salts (HA and HAS), and finally extracts from filter samples collected in a rural area (38°42′ N, 115°08′ E) close to Beijing during haze events in winter 2018 (AA1 and AA2, which differ by their pH; pH = 4.6, acidified with H_2SO_4, and 6.2, respectively). These filters were shown, by UPLC/DAD/(+/−)HESI-HRMS, to be chemically complex, with

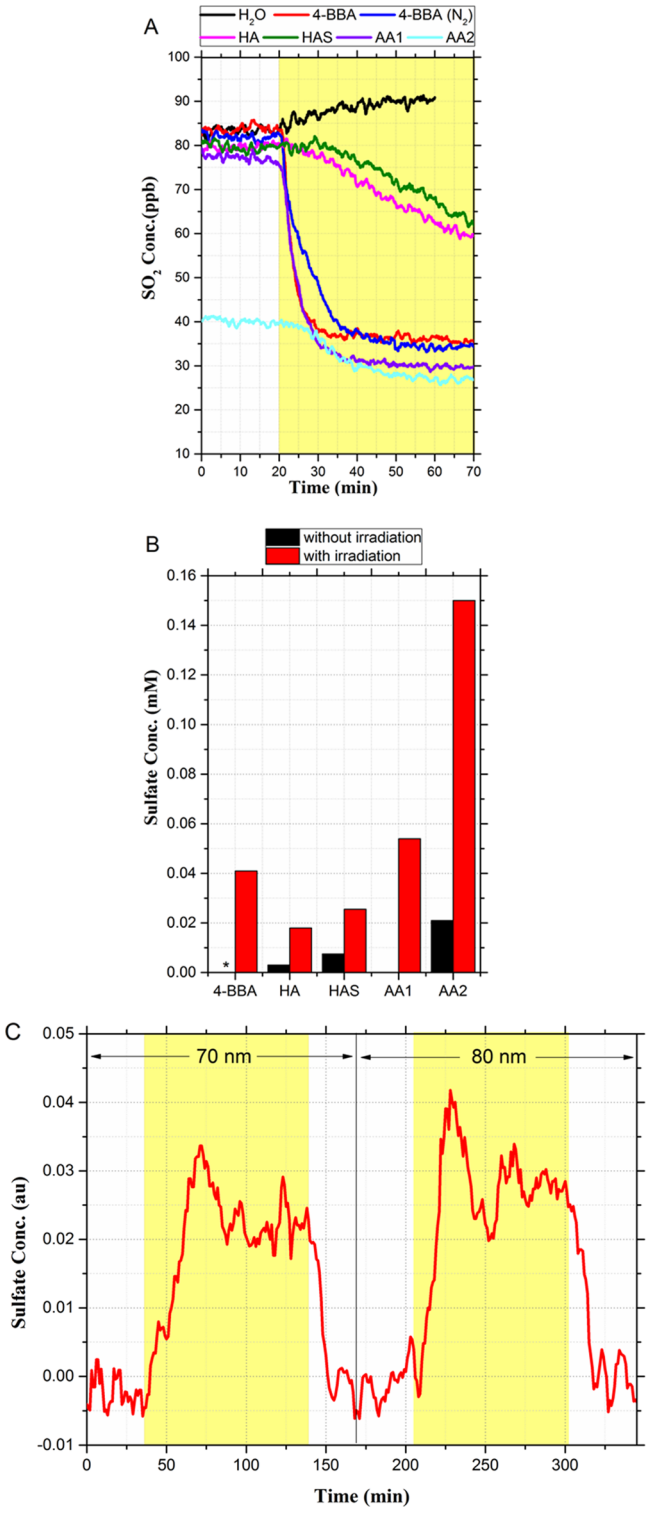

Figure 1. SO_2 loss and sulfate formation. (A) Time traces of gaseous SO_2 loss above aqueous solutions of 4-BBA, HA, HAS AA1, and AA2. (B) Corresponding sulfate production. AA1 and AA2 differ by their pH and hence their capacity to store S(IV). Sulfate concentrations were blank-corrected for the HA, HAS, AA1, and AA2 experiments. *The concentration was below the detection limit. (C) Sulfate production measured by an aerosol mass spectrometer in 4-BBA particles with diameters of 70 and 80 nm in the aerosol flow tube in a separate experiment. Residence time is 15 min.

https://dx.doi.org/10.1021/acs.est.9b06347
Environ. Sci. Technol. 2020, 54, 3114−3120

more than 70 carbonyl-containing compounds and a large amount of light-absorbing chromophoric compounds (Figure S2 and Database S1).

These solutions were initially exposed to a gaseous flow of SO_2 until steady SO_2 concentrations were reached at the outlet of the reactor, with gas-phase concentrations in the range from 40−100 ppbv. During these conditioning periods, Henry's law equilibrium and acid−base dissociation were taking place, leading to the production of hydrated SO_2, HSO_3^-, and eventually SO_3^{2-}. The product distribution is highly pH-dependent, with SO_2 being prevalent at pH < 2, HSO_3^- between 3 and 6, and finally SO_3^{2-} above pH = 7[18] (see pKa values in eqs 2 and 3).

Once the outlet gaseous SO_2 concentration was stabilized (with the exception of AA2 due to its higher pH), the light was switched on, and for all samples, we observed a sudden loss of gas-phase SO_2 associated with synchronous sulfate production in the liquid phase (see Figure 1B). Such a loss is a clear indication that light initiated the conversion of hydrated SO_2 or HSO_3^- to SO_4^{2-}, and hence the oxidation proceeds from S(IV) to S(VI).

SO_2 consumption was not observed in the absence of the photosensitizing compounds, that is, no loss on irradiated pure water. This result, combined with the poor light absorption of SO_2 in the wavelength region (λ > 295 nm) considered here, shows that in this case the triplet-state reaction of SO_2 with water plays a minor role. We attributed the loss of gaseous SO_2 to a chemical reaction between dissolved S(IV) and the photosensitizer triplet state or oxidants produced from the excited state and oxygen. In fact, it has been shown that both humic acids and 4-BBA are sources of HO_2 (and hence OH) radicals when exposed to light.[13,19] The formation of such radicals could then readily react with dissolved S(IV) and lead to the observations depicted in Figure 1. However, similar trends were observed when the carrier gas was changed to pure nitrogen and all solutions were deoxygenated. This clearly rules out the influence of secondary oxidants, produced in the solution, but points toward a direct reaction of S(IV) and the excited state of the photosensitizer.

To test whether such a sulfate production could also be observed under different conditions, we performed aerosol flow tube experiments. Here, a bulk solution containing 4-BBA was nebulized producing aerosols, and then aerosols were dried, size-selected (70 or 80 nm), and injected into the flow tube with a residence time of ∼15 min. SO_2 was injected at around 630 ppb in pure air acting as the carrier gas. At the reactor outlet, particles were chemically characterized by means of an aerosol mass spectrometer (AMS, Aerodyne), which is highly sensitive to sulfate. This is a similar approach to the one previously used for investigating photosensitized organic aerosol growth.[20] As shown by Figure 1C, once the lights were switched on, we observed a clear production of sulfate in the particle phase, similar to the bulk experiments above (note that due to the low surface-to-volume ratio, the loss of gaseous SO_2 could not be monitored in these experiments). In other words, we observed a photosensitized sulfate production, which took place within the condensed phase.

Triplet excited states are often considered as more significant excited states in photochemistry compared to the singlet excited states due to their longer lifetimes. Laser-flash illumination of some selected photosensitizers, which are simultaneously representative of those found in dissolved organic matter and biomass burning plumes (including fires for residential heating),[13] in deoxygenated aqueous solutions led to the production of the corresponding triplet state, whose decay was monitored as a function of time[21] to derive the corresponding rate constant as a function of reactant concentration, pH, and so on (as detailed below). First, the quenching rates of these triplet states were observed to be highly pH-dependent in the absence of added S(IV), with acetophenone and 4-BBA being quenched faster under more acidic conditions, but with no obvious influences on flavone and xanthone in this pH range (Figure 2A and Figure S3). In addition to highlighting their pH dependence, those trends are useful to discriminate which S(IV) species is reactive with a given T*.

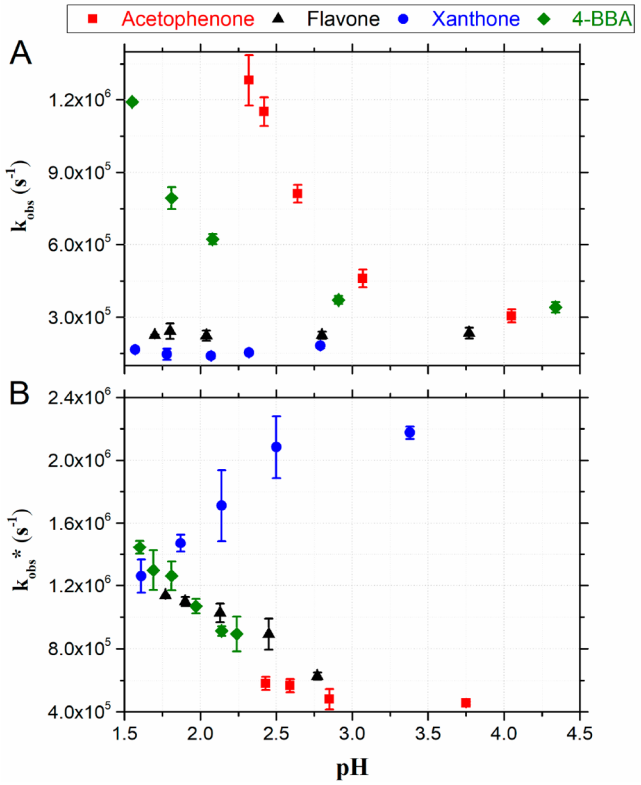

Figure 2. pH influence on the quenching rates of the triplet states in the (A) absence and (B) presence of S(IV). Red squares, acetophenone, 0.25 mM sodium sulfite; black triangles, flavone, 0.1 mM sodium sulfite; blue circles, xanthone, 1 mM sodium sulfite; green diamonds, 4-BBA, 20 mM sodium sulfite. k_{obs}* is the blank-corrected quenching rates, which means here these values obtained from the triplet states being quenched only by S(IV). It should be noted that here xanthone concentrations were different from other xanthone experiments in this study.

Figure S4 shows experiments being performed by adding sodium sulfite (Na_2SO_3) into the deoxygenated aqueous solutions, which redistributed into the other S(IV) compounds depending on pH (their distribution in solution can be calculated based on equilibrium eqs 1−3). All investigated triplet states were efficiently quenched by the presence of aqueous S(IV) species but exhibited different quenching rates (see Figure 2B and 3). Figure 2B shows the quenching rates of the triplet states in the presence of the same concentration of S(IV) but at different pH values, that is, with a different speciation between hydrated SO_2 and HSO_3^-. Taking into account the trends shown in Figure 2A, these results indicate that the triplet state of flavone is more reactive toward hydrated

https://dx.doi.org/10.1021/acs.est.9b06347
Environ. Sci. Technol. 2020, 54, 3114−3120

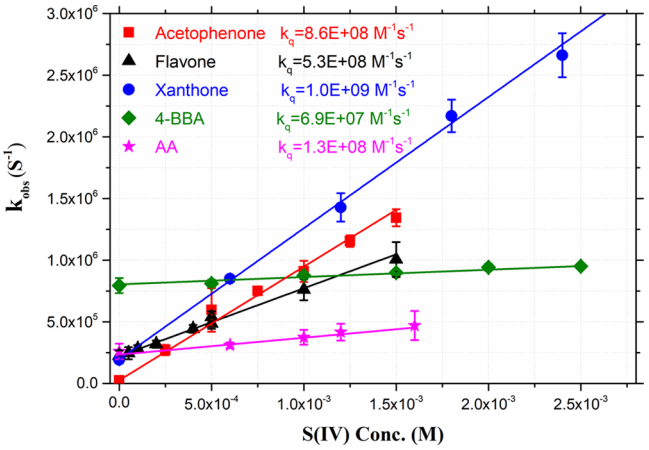

Figure 3. Stern–Volmer plots of the observed quenching first-order rate coefficients k_{obs} as a function of aqueous S(IV) concentration. Red squares, acetophenone; black triangles, flavone; blue circles, xanthone; green diamonds, 4-BBA; pink stars, HULIS-AA. The pH of all acetophenone solutions is 2.6, and the pH of all flavone, xanthone, 4-BBA, and HULIS-AA solutions is 1.8.

SO_2, while xanthone is more reactive toward HSO_3^- (see Table S1). However, the triplet states of acetophenone and 4-BBA were quenched faster under more acidic solutions as they are more reactive under acidic conditions (see Figure 2A) and also probably more reactive toward hydrated SO_2.

In the investigated pH range, both hydrated SO_2 and HSO_3^- were quenching or reacting with T*. Figure 3 shows a Stern–Volmer plot of the measured quenching rates under acidic conditions where hydrated SO_2 and HSO_3^- are dominant. In order to simplify the kinetics treatment, we assumed that both S(IV) species are reacting at the same rate with the triplet state. In such a simplified system, the observed quenching rate should depend linearly on the total aqueous S(IV) concentration (see Figure 3). The measured second-order rate constants were all in an excess of 6×10^7 M^{-1} s^{-1}, with 4-BBA being the slowest (6.9×10^7 M^{-1} s^{-1}) and xanthone the fastest (1.0×10^9 M^{-1} s^{-1}). The extracts of the ambient filters from an authentic Chinese haze event also showed a reactive triplet state and quenched by S(IV) with a rate constant of 1.3×10^8 M^{-1} s^{-1} (see Figure 3).

DISCUSSION

These observations can only be explained by a direct reaction between S(IV) species and the studied triplet states (T*) as the organic photodissociation is not occurring under our experimental conditions with well-defined photosensitizers. The possible reaction pathways are listed below:

$$SO_2(aq) + T^* \rightarrow SO_2^* + T;\ \text{energy transfer (a)}$$

$$SO_2(aq) + T^* \rightarrow SO_2^{\bullet+} + T^{\bullet-};\ \text{electron transfer to T* (b)}$$

$$SO_2(aq) + T^* \rightarrow SO_2^{\bullet-} + T^{\bullet+};\ \text{electron transfer from T* (c)}$$

$$HSO_3^- + T^* \rightarrow HSO_3^{\bullet} + T^{\bullet-};\ \text{electron transfer to T* (d)}$$

$$HSO_3^- + T^* \rightarrow SO_3^{\bullet-} + HT^{\bullet};\ \text{hydrogen transfer to T* (e)}$$

All these initiation reactions produce sulfur-containing transient compounds that will start chain reactions and decay to sulfate. While we cannot, from our observations, be fully conclusive on the exact reaction mechanism, one could still discuss the plausibility of each pathway. Let us consider 4-BBA as a model photosensitizer for which some information is known (in contrast for instance to the authentic aerosol samples). The energy of the triplet of 4-BBA (~290 kJ mol^{-1})[13] is slightly lower than the triplet energy of SO_2 (~300 kJ mol^{-1}),[7] which cannot lead to an efficient (if any) energy transfer in this case. However, one cannot rule out that for higher triplet states, energy transfer could lead to a significant yield of excited-state SO_2 (pathway (a)) that would then react more efficiently with water, producing OH radicals and therefore leading to the observed oxidation process.[9] An electron transfer, either way, would therefore be the prominent pathway. SO_2 has a zwitterion structure, where the sulfur is positively charged, which would prevent any significant electron transfer from its electron lone pairs. However, if produced through pathway (b), $SO_2^{\bullet+}$ might react directly with water and initiate some further radical and oxidative chemistry.[22] Another possibility is an electron transfer to SO_2 producing $SO_2^{\bullet-}$. It was however not possible to observe the transient spectra of $SO_2^{\bullet-}$, nor of the associated ketyl radical produced in pathway (c), as the absorption of the radical anion overlapped with that of the organic photosensitizer. $SO_2^{\bullet-}$ has been previously reported to be highly reactive in aqueous solutions, undergoing several reaction pathways including reactions with oxygen and typical S(IV) species, ending in the production of sulfate.[23−25] In addition, HSO_3^- could also either transfer the electron to T* producing $HSO_3^{\bullet}$ (d) or a H-atom producing $SO_3^{\bullet-}$ (e), which could also continue to react with oxygen and other S(IV) species to produce sulfate.[23] This reaction scheme would probably explain the measured quenching rates.

While the exact pathway is uncertain, the reaction rates are however established via the kinetics observations discussed above. If we assume that the reaction between S(IV) and T* is the rate-limiting step and the rate coefficient is pH-independent, then one can derive the associated sulfate formation rates. The pH independence arises from the assumption made that both hydrated SO_2 and HSO_3^- have similar reactivities and that the total aqueous S(IV) concentration can be used as a reasonable proxy, leading to the linearity shown in Figure 3. Details about these calculations are given in the Supporting Information. It also should be noted that here particles were assumed to be homogeneously mixed and in a liquid state. This chemistry (reactions a–e) may then induce a significant S(IV) oxidation in wet aerosols when both SO_2 and particle phase photosensitizer, such as HULIS,[14] levels are high. Such conditions are typically observed during Asian haze events, which combine high humidity and significant anthropogenic emissions from residential burning, with a contribution of up to 20 wt % during haze events. By updating the scenario of Cheng et al.[10] to take into account high H_2O_2 levels recently reported,[26] we estimated the sulfate formation rate associated with SO_2 reacting with O_3, H_2O_2, TMIs, NO_2, and T* (using 1.3×10^8 M^{-1} s^{-1} as obtained from the authentic samples) (Figure 3). It should be noted again that we assumed that the triplet states are reactive toward all S(IV) species (hydrated SO_2 and HSO_3^-) and independent of their actual pH speciation (eqs 1–3). To estimate the sulfate formation rate under the scenario set by Cheng et al.,[10] we do need to estimate the particle phase concentration of triplet states under steady-state haze daylight conditions. Clearly, the data related to this quantity are very limited. For instance, Kaur et al.[27] reported very recently on such concentrations for some cleaner conditions encountered in California but with large uncertainty. Meanwhile, several studies investigated the amount of singlet oxygen and its ratio to coexisting triplet states in the range approximately 1,[10] 3,[28] and 10–100,[27] respectively.

https://dx.doi.org/10.1021/acs.est.9b06347
Environ. Sci. Technol. 2020, 54, 3114−3120

Altogether, this leads to estimated concentrations in the range from 2.3×10^{-13} to 1.6×10^{-10} M.[27] Using this range of concentrations leads to the estimated sulfate production rates shown in Figure 4. Overall, these results show that the photosensitizing pathway could make a significant contribution to the sulfate formation (Figure 4). In the pH range from 4 to 6, which overlaps with the conditions of Chinese haze,[29,30] the sulfate production rates are in the range of 1.1×10^{-4} - 7.9 μg m^{-3} h^{-1}. This is a new finding that not only will help close gaps between field observations and numerical models but also may help in defining new regulations to reduce sulfate formation and hence the harmful effects of these haze events. Overall, this study also stresses the knowledge gap around particle phase concentration of photosensitizing compounds and the associated quantum yield for triplet-state formation.

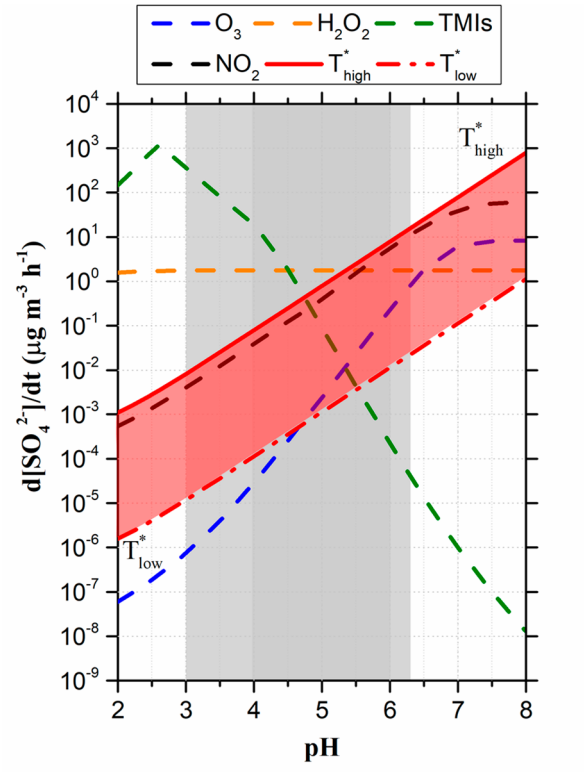

Figure 4. Sulfate production rates for Beijing winter haze calculated for main aqueous-phase reaction pathways versus pH. The blue, orange, green, and black lines represent O_3, H_2O_2, TMIs, and nitrogen dioxide (NO_2) pathways, respectively, from Cheng et al.[10] The red region represents the photosensitized oxidation. Gray-shaded areas indicate characteristic pH ranges during haze episodes in China, with the darker ones being more common.[29,30]

■ ASSOCIATED CONTENT

Supporting Information

The Supporting Information is available free of charge at https://pubs.acs.org/doi/10.1021/acs.est.9b06347.

Additional experimental details, 4 figures, 3 tables and dataset S1 were given.

Schematic of the pulsed laser excitation system; UPLC-DAD absorption and ion chromatograms of the chromophores in ambient aerosols; transient absorption decays of the triplet states of acetophenone, flavone, xanthone, 4-BBA, and ambient aerosol extracts; tables of rate coefficients for the quenching processing and parameter settings used for processing the LC-MS raw data; and database of the formula lists of organic compounds in ambient aerosol samples (PDF)

■ AUTHOR INFORMATION

Corresponding Authors

Jianmin Chen − *Shanghai Key Laboratory of Atmospheric Particle Pollution and Prevention (LAP3), Department of Environmental Science & Engineering, Institute of Atmospheric Sciences, Fudan University, Shanghai 200438, China; Institute of Eco-Chongming, Shanghai 200062, China;* orcid.org/0000-0001-5859-3070; Email: jmchen@fudan.edu.cn

Christian George − *Univ Lyon, Université Claude Bernard Lyon 1, CNRS, IRCELYON, F-69626 Villeurbanne, France;* orcid.org/0000-0003-1578-7056; Email: christian.george@ircelyon.univ-lyon1.fr

Authors

Xinke Wang − *Univ Lyon, Université Claude Bernard Lyon 1, CNRS, IRCELYON, F-69626 Villeurbanne, France*

Rachel Gemayel − *Univ Lyon, Université Claude Bernard Lyon 1, CNRS, IRCELYON, F-69626 Villeurbanne, France*

Nathalie Hayeck − *Univ Lyon, Université Claude Bernard Lyon 1, CNRS, IRCELYON, F-69626 Villeurbanne, France*

Sebastien Perrier − *Univ Lyon, Université Claude Bernard Lyon 1, CNRS, IRCELYON, F-69626 Villeurbanne, France*

Nicolas Charbonnel − *Univ Lyon, Université Claude Bernard Lyon 1, CNRS, IRCELYON, F-69626 Villeurbanne, France*

Caihong Xu − *Shanghai Key Laboratory of Atmospheric Particle Pollution and Prevention (LAP3), Department of Environmental Science & Engineering, Institute of Atmospheric Sciences, Fudan University, Shanghai 200438, China*

Hui Chen − *Shanghai Key Laboratory of Atmospheric Particle Pollution and Prevention (LAP3), Department of Environmental Science & Engineering, Institute of Atmospheric Sciences, Fudan University, Shanghai 200438, China*

Chao Zhu − *Shanghai Key Laboratory of Atmospheric Particle Pollution and Prevention (LAP3), Department of Environmental Science & Engineering, Institute of Atmospheric Sciences, Fudan University, Shanghai 200438, China*

Liwu Zhang − *Shanghai Key Laboratory of Atmospheric Particle Pollution and Prevention (LAP3), Department of Environmental Science & Engineering, Institute of Atmospheric Sciences, Fudan University, Shanghai 200438, China;* orcid.org/0000-0002-0765-8660

Lin Wang − *Shanghai Key Laboratory of Atmospheric Particle Pollution and Prevention (LAP3), Department of Environmental Science & Engineering, Institute of Atmospheric Sciences, Fudan University, Shanghai 200438, China;* orcid.org/0000-0002-4905-3432

Sergey A. Nizkorodov − *Department of Chemistry, University of California, Irvine, Irvine, California 92697, United States;* orcid.org/0000-0003-0891-0052

Xinming Wang − *State Key Laboratory of Organic Geochemistry and Guangdong province Key Laboratory of Environmental Protection and Resources Utilization, Guangzhou Institute of Geochemistry, Chinese Academy of Sciences, Guangzhou 510640, China;* orcid.org/0000-0002-1982-0928

Zhe Wang − *Department of Civil and Environmental Engineering, The Hong Kong Polytechnic University, Hong Kong 999077, China*

https://dx.doi.org/10.1021/acs.est.9b06347
Environ. Sci. Technol. 2020, 54, 3114−3120

Tao Wang − *Department of Civil and Environmental Engineering, The Hong Kong Polytechnic University, Hong Kong 999077, China*
Abdelwahid Mellouki − *Institut de Combustion, Aérothermique, Réactivité et Environnement (ICARE), CNRS/OSUC, 45071 Orléans, France*
Matthieu Riva − *Univ Lyon, Université Claude Bernard Lyon 1, CNRS, IRCELYON, F-69626 Villeurbanne, France;* orcid.org/0000-0003-0054-4131

Complete contact information is available at: https://pubs.acs.org/10.1021/acs.est.9b06347

Funding

This project was supported by the ANR-RGC program (project ANR-16-CE01-0013, A-PolyU502/16), the European Union's Horizon 2020 research and innovation program under grant agreement no. 690958 (MARSU), the Ministry of Science and Technology of China (2016YFC0202700), the National Natural Science Foundation of China (91843301 and 91743202), and the National research program for key issues in air pollution control (DQGG0103 and DQGG0102). S.N. thanks the Université Claude Bernard Lyon 1 for providing him with a visiting professorship in the summer of 2018. C.G. thanks Kristopher McNeil for very helpful discussions and comments on the reaction mechanism.

Notes

The authors declare no competing financial interest.
All data to support the conclusions of this manuscript are included in the main text and Supporting Information.

REFERENCES

(1) Albrecht, B. A. Aerosols, Cloud Microphysics, and Fractional Cloudiness. *Science* **1989**, *245*, 1227−1230.
(2) Sedlak, D. L.; Hoigne, J. Oxidation of S(IV) in Atmospheric Water by Photooxidants and Iron in the Presence of Copper. *Environ. Sci. Technol.* **1994**, *28*, 1898−1906.
(3) Warneck, P. *Chemistry of the Natural Atmosphere*; Academic Press: 2000.
(4) Guo, S.; Hu, M.; Zamora, M. L.; Peng, J.; Shang, D.; Zheng, J.; Du, Z.; Wu, Z.; Shao, M.; Zeng, L.; Molina, M. J.; Zhang, R. Elucidating severe urban haze formation in China. *Proc. Natl. Acad. Sci. U. S. A.* **2014**, *111*, 17373−17378.
(5) Wang, Y.; Zhang, Q.; Jiang, J.; Zhou, W.; Wang, B.; He, K.; Duan, F.; Zhang, Q.; Philip, S.; Xie, Y. Enhanced sulfate formation during China's severe winter haze episode in January 2013 missing from current models. *J. Geophys. Res.: Atmos.* **2014**, *119*, 10,425−10,440.
(6) Hung, H.-M.; Hoffmann, M. R. Oxidation of Gas-Phase SO_2 on the Surfaces of Acidic Microdroplets: Implications for Sulfate and Sulfate Radical Anion Formation in the Atmospheric Liquid Phase. *Environ. Sci. Technol.* **2015**, *49*, 13768−13776.
(7) Donaldson, D. J.; Kroll, J. A.; Vaida, V. Gas-phase hydrolysis of triplet SO_2: A possible direct route to atmospheric acid formation. *Sci. Rep.* **2016**, *6*, 30000.
(8) Kroll, J. A.; Frandsen, B. N.; Kjaergaard, H. G.; Vaida, V. Atmospheric Hydroxyl Radical Source: Reaction of Triplet SO_2 and Water. *J. Phys. Chem. A* **2018**, *122*, 4465−4469.
(9) Martins-Costa, M. T. C.; Anglada, J. M.; Francisco, J. S.; Ruiz-López, M. F. Photochemistry of SO_2 at the Air−Water Interface: A Source of OH and HOSO Radicals. *J. Am. Chem. Soc.* **2018**, *140*, 12341−12344.
(10) Cheng, Y.; Zheng, G.; Wei, C.; Mu, Q.; Zheng, B.; Wang, Z.; Gao, M.; Zhang, Q.; He, K.; Carmichael, G.; Pöschl, U.; Su, H. Reactive nitrogen chemistry in aerosol water as a source of sulfate during haze events in China. *Sci. Adv.* **2016**, *2*, e1601530.
(11) Li, L.; Hoffmann, M. R.; Colussi, A. J. Role of Nitrogen Dioxide in the Production of Sulfate during Chinese Haze-Aerosol Episodes. *Environ. Sci. Technol.* **2018**, *52*, 2686−2693.
(12) George, C.; Ammann, M.; D'Anna, B.; Donaldson, D. J.; Nizkorodov, S. A. Heterogeneous Photochemistry in the Atmosphere. *Chem. Rev.* **2015**, *115*, 4218−4258.
(13) McNeill, K.; Canonica, S. Triplet state dissolved organic matter in aquatic photochemistry: reaction mechanisms, substrate scope, and photophysical properties. *Environ. Sci.: Processes Impacts* **2016**, *18*, 1381−1399.
(14) Baduel, C.; Monge, M. E.; Voisin, D.; Jaffrezo, J.-L.; George, C.; El Haddad, I.; Marchand, N.; D'Anna, B. *Environ. Sci. Technol.* **2011**, *45*, 5238.
(15) Ciuraru, R.; Fine, L.; van Pinxteren, M.; D'Anna, B.; Herrmann, H.; George, C. Photosensitized production of functionalized and unsaturated organic compounds at the air-sea interface. *Sci. Rep.* **2015**, *5*, 12741.
(16) Dupart, Y.; King, S. M.; Nekat, B.; Nowak, A.; Wiedensohler, A.; Herrmann, H.; David, G.; Thomas, B.; Miffre, A.; Rairoux, P.; D'Anna, B.; George, C. Mineral dust photochemistry induces nucleation events in the presence of SO_2. *Proc. Natl. Acad. Sci.* **2012**, *109*, 20842−20847.
(17) Jammoul, A.; Dumas, S.; D'Anna, B.; George, C. Photoinduced oxidation of sea salt halides by aromatic ketones: a source of halogenated radicals. *Atmos. Chem. Phys.* **2009**, *9*, 4229−4237.
(18) Seinfeld, J. H.; Pandis, S. N. *Atmospheric Chemistry and Physics: From Air Pollution to Climate Change*; Wiley: 2006.
(19) Canonica, S.; Jans, U.; Stemmler, K.; Hoigne, J. *Environ. Sci. Technol.* **1995**, *29*, 1822.
(20) Monge, M. E.; Rosenorn, T.; Favez, O.; Muller, M.; Adler, G.; Abo Riziq, A.; Rudich, Y.; Herrmann, H.; George, C.; D'Anna, B. Alternative pathway for atmospheric particles growth. *Proc. Natl. Acad. Sci. U. S. A.* **2012**, *109*, 6840−6844.
(21) Tinel, L.; Rossignol, S.; Ciuraru, R.; Dumas, S.; George, C. Photosensitized reactions initiated by 6-carboxypterin: singlet and triplet reactivity. *Phys. Chem. Chem. Phys.* **2016**, *18*, 17105−17115.
(22) Cartoni, A.; Catone, D.; Bolognesi, P.; Satta, M.; Markus, P.; Avaldi, L. HSO_2^+ Formation from Ion-Molecule Reactions of $SO_2^{\bullet+}$ with Water and Methane: Two Fast Reactions with Reverse Temperature-Dependent Kinetic Trend. *Chem. − Eur. J.* **2017**, *23*, 6772−6780.
(23) Neta, P.; Huie, R. E.; Harriman, A. One-electron-transfer reactions of the couple SO_2/SO_2^- in aqueous-solutions. pulse radiolytic and cyclic voltammetric studies. *J. Phys. Chem.* **1987**, *91*, 1606−1611.
(24) Burlamacchi, L.; Guarini, G.; Tiezzi, E. Mechanism of decomposition of sodium dithionite in aqueous solution. *Trans. Faraday Soc.* **1969**, *65*, 496−502.
(25) Rinker, R. G.; Gordon, T. P.; Mason, D. M.; Sakaida, R. R.; Corcoran, W. H. Kinetics and mechanism of the air oxidation of the dithionite ion ($S_2O_4^=$) in aqueous solution. *J. Phys. Chem.* **1960**, *64*, 573−581.
(26) Ye, C.; Liu, P.; Ma, Z.; Xue, C.; Zhang, C.; Zhang, Y.; Liu, J.; Liu, C.; Sun, X.; Mu, Y. High H_2O_2 Concentrations Observed during Haze Periods during the Winter in Beijing: Importance of H_2O_2 Oxidation in Sulfate Formation. *Environ. Sci. Technol. Lett.* **2018**, *5*, 757−763.
(27) Kaur, R.; Labins, J. R.; Helbock, S. S.; Jiang, W.; Bein, K. J.; Zhang, Q.; Anastasio, C. Photooxidants from Brown Carbon and Other Chromophores in Illuminated Particle Extracts. *Atmos. Chem. Phys.* **2019**, *19*, 6579−6594.
(28) Kaur, R.; Anastasio, C. First Measurements of Organic Triplet Excited States in Atmospheric Waters. *Environ. Sci. Technol.* **2018**, *52*, 5218−5226.
(29) Song, S.; Gao, M.; Xu, W.; Shao, J.; Shi, G.; Wang, S.; Wang, Y.; Sun, Y.; McElroy, M. B. Fine-particle pH for Beijing winter haze as inferred from different thermodynamic equilibrium models. *Atmos. Chem. Phys.* **2018**, *18*, 7423−7438.
(30) Ding, J.; Zhao, P.; Su, J.; Dong, Q.; Du, X. Aerosol pH and its influencing factors in Beijing. *Atmos. Chem. Phys. Discuss.* **2018**, *2018*, 1−34.